PHYSICAL REVIEW A VOLUME 58, NUMBER 1 JULY 1998

Precision microwave measurement of the $2\,^3P_1-2\,^3P_0$ interval in atomic helium

C. H. Storry and E. A. Hessels
Department of Physics, York University, 4700 Keele Street, Toronto, Ontario, Canada M3J 1P3

(Received 10 March 1998)

We have measured the $2\,^3P_1-2\,^3P_0$ interval in atomic helium to be 29 616.966(13) MHz (an accuracy of 400 ppb). The microwave transition is driven using a laser-excited thermal beam of metastable helium atoms. The result of the measurement resolves the discrepancy between a previous, less-precise microwave measurement and recent laser measurements of this interval. Comparison of measured and theoretical predictions for this interval allows for a determination of the fine-structure constant. [S1050-2947(98)50707-X]

PACS number(s): 31.30.Jv, 32.30.Bv

The $n=2$ triplet P fine-structure intervals in atomic helium have long been recognized as important for the testing of quantum electrodynamics and for measuring the fine-structure constant. The fact that the $2\,^3P$ states are relatively long lived (with a lifetime of 98 ns) allows for high-precision measurements of the large (approximately 30 GHz) fine-structure intervals. High-precision theoretical predictions were first made by Douglas and co-workers [1] and, recently, even higher-precision theory has been introduced by Drake and co-worker [2]. On the experimental side, a series of precision microwave measurements were done by Hughes and co-workers [3], and, more recently, the intervals have been determined from precision laser measurements of the $2\,^3S-2\,^3P$ intervals [4–6]. These laser measurements are in disagreement with the earlier microwave measurements. We present here a high-precision microwave measurement.

A schematic of the technique used for this measurement is shown in Fig. 1. A dense thermal beam of metastable helium atoms (5×10^{14}/sr s) is created in a discharge source similar to that described in Ref. [7]. A small dc magnetic field (8.9 or 25.6 G) is applied to separate the energies of the different m substrates of the $2\,^3S$ and $2\,^3P$ states, as shown in Fig. 1. First, a 1.08-μm diode laser (A in Fig. 1), which is linearly polarized in the direction of the dc magnetic field, empties the $2\,^3S_1$ $m=0$ metastable state by driving the $2\,^3S_1$ $m=0$ to $2\,^3P_0$ transition. The $2\,^3P_0$ state decays back to the $2\,^3S$ state, with equal probability of decaying into each of the three m substates. In the approximately 6 μs that the atoms spend in this 1-cm-wide laser beam, they undergo approximately 30 cycles of this transition, reducing the $2\,^3S$ $m=0$ population by more than 99.5%. Next, a second 1.08-μm laser (B in Fig. 1), this one linearly polarized perpendicular to the direction of the magnetic field, is tuned to excite the $2\,^3S_1$ $m=1$ population up to the $2\,^3P_1$ $m=0$ state. This $m=0$ state decays back down to the $2\,^3S_1$ $m=1$ and $m=-1$ states, but is forbidden to decay down to the $2\,^3S_1$ $m=0$ state, and thus the $2\,^3S_1$ $m=0$ state remains empty.

Immediately following this laser excitation, the atoms enter a section of WR28 waveguide (C in Fig. 1), where a microwave field drives the $2\,^3P_1$ $m=0$ to $2\,^3P_0$ $m=0$ magnetic-dipole transition. The thermal atoms travel a distance of only about 0.2 mm within a $2\,^3P$ lifetime, and thus it is necessary that the waveguide be very close to the excitation laser beam. To accomplish this, the excitation laser beam is focused to a waist size 30 μm wide (and 4 mm high). 1.6-mm holes in the narrow 3.56-mm dimensions of the waveguide allow the atoms to pass through. The wall thickness of the waveguide is 1.02 mm, and this is reduced to 0.13 mm at the entrance hole. 25-μm-diam stainless-steel wires are stretched across this hole, as shown in Fig. 1, in order to contain the microwave fields to inside of the waveguide. 16 (and later 32) wires are used, leaving an average spacing of 75 (and later 25) μm between the wires.

After the $2\,^3P_1-2\,^3P_0$ microwave transition is driven, the $2\,^3P_0$ atoms decay equally into all three m states of the $2\,^3S$ state, including the $m=0$ state. Thus, driving the microwave transition results in a repopulation of the previously emptied $m=0$ state. This repopulation is detected 16 cm down the beamline by laser exciting the $m=0$ metastables up to the $2\,^3P_0$ state (D in Fig. 1) and observing the resulting fluorescence. A 7.6-cm parabolic mirror (with 2.9-cm focal length) and a Fresnel lens focus the light onto a liquid-nitrogen-cooled InGaAs photodiode. Less than 10% of the total fluorescing light can be focused onto the 3-mm-diam photodiode, which has a quantum efficiency of 90%. A lock-in amplifier extracts the photodiode signal synchronous with the 100% amplitude modulation of the microwave power.

The resulting signal as a function of microwave frequency is shown in Fig. 2. The final uncertainty in the measurement is dominated by systematic effects, as discussed in the following paragraphs. A summary of the line centers obtained from the data is shown in Table I.

The first systematic effect is due to microwave fields that leak out of the 1.6-mm entrance hole in the waveguide. The size of these fields is greatly reduced by the presence of the 25-μm wires. The leakage fields consist of both fields that radiate out of the hole and those that bulge out between the wires but continue to travel down the waveguide. The first

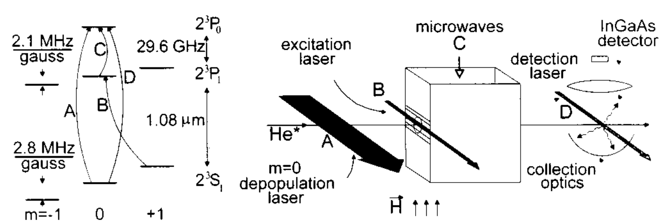

FIG. 1. Energy-level diagram and schematic of the experimental setup. Details are given in the text.

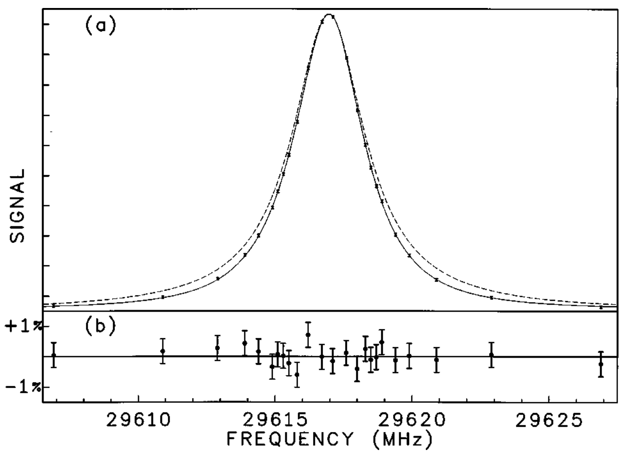

FIG. 2. (a) Typical data for the microwave resonance. The TDPT model described in the text (solid line) gives a good fit to the data (points with error bars), whereas the naive Lorentzian (dashed line) gives a very poor fit. (b) The residuals (experimental data minus solid line) are shown on an expanded scale at the bottom of the plot.

causes shifts in our resonance because the direction of propagation of the radiated fields leads to Doppler shifts and because the radiated waves experience a phase shift as they pass by the wires. The second type of field causes no shift, and the amplitude of this field is expected to decay exponentially outside of the waveguide. The effects due to both leakage fields on the line shape and line center can be calculated using time-dependent perturbation theory (TDPT). The probability of repopulating the $2\,^3S$ $m=0$ state is [8]

TABLE I. Measured line centers. The second column gives the line centers obtained from extrapolations, as shown in Fig. 3. The values in parentheses are one standard deviation uncertainties in the last digits. The first uncertainty is from the extrapolation, and the 4-kHz uncertainty is due to Doppler shifts (1.2 kHz), light shifts (2 kHz), and microwave power variation (3.5 kHz). The third column is the quadratic Zeeman shift, and the final column gives the corrected centers. Centers are given for the two magnetic fields, the two numbers of stainless-steel wires, the two excitation laser powers, and for the two nominally identical repetitions of the data taken during different months. In each case, the center given is the average obtained from all of the data that were taken with the experimental parameters listed in column 1. The final row uses the average of all data taken and gives the final measured value for the center. All values are in kHz.

Experimental setup	Extrapolated line center	Zeeman shift	Measured center
$B=8.9$ G	29 616 954(12)(4)	16(0)	29 616 970(13)
$B=25.6$ G	29 616 832(13)(4)	130(2)	29 616 962(14)
16 wires	29 616 897(13)(4)	73(1)	29 616 970(14)
32 wires	29 616 888(12)(4)	73(1)	29 616 961(13)
10% laser power	29 616 890(12)(4)	73(1)	29 616 963(13)
100% laser power	29 616 895(13)(4)	73(1)	29 616 968(14)
Data set No. 1	29 616 888(12)(4)	73(1)	29 616 961(13)
Data set No. 2	29 616 898(16)(4)	73(1)	29 616 971(17)
All data	29 616 893(12)(4)	73(1)	29 616 966(13)

$$\int_{t=-t_b}^{\infty} |b(t)|^2 \Gamma e^{-\Gamma t} dt,$$

where C is a normalization constant, $\Gamma=10.216\times10^6\ \mathrm{s}^{-1}$ is the $2\,^3P$ decay rate [9] and $|b(t)|$ is the amplitude for making the microwave transition:

$$|b(t)| = \frac{\mu_0}{\sqrt{6}\hbar}\left|\int_{t'=-t_b}^{t} e^{i\Delta\omega t'} H_z(t')dt'\right|,$$

where $\mu_0 H_z/\sqrt{6}$ is the magnetic-dipole matrix element, and the z component of the microwave magnetic field is

$$H_z(t) = H_0\left(1 - \frac{e^{-t/t_a}}{2}\right)\cos(\omega t) \quad \text{for } t>0,$$

$$H_0\left(\frac{e^{t/t_a}}{2}\cos(\omega t) + \epsilon\cos[\omega(1+\beta)t - \phi]\right) \quad \text{for } t<0,$$

which includes both the radiating field (the term proportional to ϵ) and the exponentially decaying nonradiating field. Here, ω is the angular frequency of the microwave field, ϵ and ϕ are the relative amplitude and phase of the radiated microwaves (compared to those inside the waveguide), $\beta=v/c$, $t_a=a/v$, and $t_b=b/v$, where v is the velocity of the atom, a is the exponential decay distance for the nonradiating fields, and b is the distance between the laser excitation and the waveguide entrance hole. The full line shape is obtained by integrating over the atomic-beam velocity distribution.

The analytic expression for the result of the TDPT calculation is lengthy, but straightforward to calculate. The solid line in Fig. 2 is an example of the line shape. The dashed curve in that figure is the Lorentzian line shape (with full width at half maximum of $\Gamma/\pi=3.252$ MHz), which would be present if the leakage fields were zero. It is clear from the plot that the leakage fields play an important role. The residuals (experimental data minus model line shape) shown at the bottom of the figure show excellent agreement between the data and the TDPT shape. Other trial line shapes (e.g., a Lorentzian with its center and width floating) do not give acceptable agreement.

To further study the effects of the leakage fields, data are taken with different distances (b) between the excitation laser and the waveguide entrance hole. The amplitude of the microwave signal shows the expected exponential decrease with distance due to the lifetime of the $2\,^3P_1$ state and indicates that the average speed for the atoms is approximately 2000 m/s, as expected [7]. Figure 3 shows plots of the experimental width and observed line center versus b. The solid curves in these plots are the predictions from the TDPT model. The choice of a, ϕ, ϵ, and b_0 (the excitation-laser-to-waveguide distance for the points at $x=0$ in Fig. 3) is determined by finding the best fit of these parameters to the data of Fig. 3. Γ is not varied in the fit. The least-squares fit constrains all four parameters: $a=60(10)$ μm, $\phi=25(5)°$, $b_0=150(30)$ μm, and $\epsilon=0.055(5)$ for 16 wires; and $a=40(10)$ μm, $\phi=25(5)°$, $b_0=150(30)$ μm, and $\epsilon=0.045(5)$ for 32 wires. The fit values for ϵ imply that approximately 2×10^{-4} of the waveguide power is radiated out of the hole. The two values of a seem reasonable given the

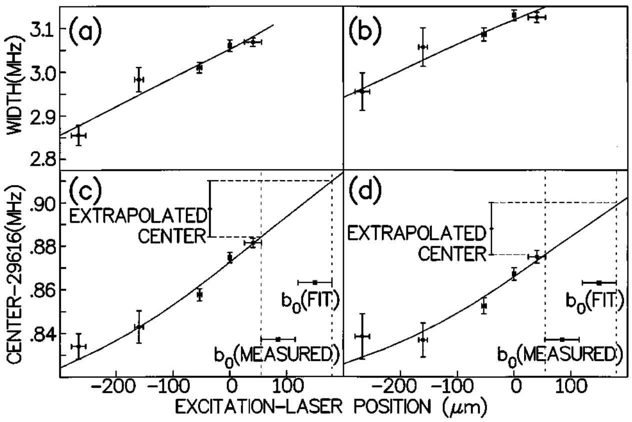

FIG. 3. Variation of line centers and linewidths with the position of the excitation laser for 16-wire data [(a) and (c)] and 32-wire data [(b) and (c)]. The solid line is from the TDPT predictions described in the text. The line centers must be extrapolated to where the phase-shifted power radiated out of the microwave hole originates, which is determined either from the fit of these curves to the TDPT model [b_0(FIT)] or from the measured position of the wires [b_0(MEASURED)]. The extrapolated line centers are also shown.

25- and 75-μm spacing between the 25-μm wires. As expected, b_0 is the same for both numbers of wires, although it is somewhat larger than the measured distance of 85(30) μm. The fitted values imply, as expected, that both types of leakage field are smaller when the spacing between the stainless-steel wires is reduced.

The success of the TDPT model in describing the shifts and the widths of the microwave resonance as b is varied (Fig. 3) and the fact that the model predicts reasonable values for the four parameters a, ϕ, ϵ, and b_0, and its success in obtaining a good fit to the experimental line shape (Fig. 2) indicate that the model describes the physical process responsible for the shifts in our microwave resonance. As b goes to zero, the shift of the microwave resonance will also go to zero. Thus, to obtain the unshifted center, one must extrapolate the curves in Fig. 3 to the position of the waveguide entrance hole (or, more precisely, the point where the phase-shifted radiated power originates). It would seem apparent that this phase-shifted radiation originates at the 25-μm wires, and thus one should extrapolate to the measured position of these wires: 85(30) μm. The fit values for b_0 indicate that perhaps the extrapolation should extend somewhat further, to 150(30) μm. This difference may be due to the inadequacy of our model in fully describing the shifts, but we choose to include the possibility that the point of phase shift may be inside the wires and expand our error bars to include extrapolations back to both of these points. The extrapolated centers are shown in the first column of Table I along with the uncertainties in the extrapolations.

In the discussion thus far, it has been implicitly assumed that the microwave power is small enough to allow us to use TDPT. This is in fact the case for the 1 W of power present in the waveguide, which leads to a microwave magnetic field of 0.2 G. This power is well below saturation, leading to only a 2% probability of driving the $2\,^3P_1$–$2\,^3P_0$ transition. The ac Stark shift and Bloch-Siegert shift are less than 0.1 kHz and can be ignored. Power broadening is less than 1% and its effect on the extrapolations is negligible.

Since the microwaves in the waveguide propagate perpendicular to the thermal beam, Doppler shifts are small. The spread of the atomic beam is ± 3 mrad and the waveguide is perpendicular to all atoms in the atomic beam to better than 5 mrad, leading to the uncertainty of 1.2 kHz included in Table I. It is possible that the wave in the waveguide slightly distorts as it passes by the entrance hole. To ensure that no net Doppler shift could result from such a distortion, we are careful to ensure that the atomic beam fills the hole symmetrically and that the atoms that contribute to the microwave signal also fill the hole symmetrically.

Laser light shifts due to the slight overlap of the excitation laser and microwave fields is another major concern. The 25-μm wires and the tight focus of the laser help to minimize this overlap. To test for possible light shifts, approximately half of the data are taken at 90% lower excitation-laser power. The line centers obtained at the two laser powers are nearly identical. We have included an uncertainty of 2 kHz in Table I to account for possible light shifts.

Because the microwaves drive a $\Delta m=0$ transition, there is no linear Zeeman shift. There is, however, a quadratic shift [10] of 0.1977 kHz/G^2. The dc magnetic field is produced by two rectangular coils and is measured using two separate gauss meters (each accurate to better than 2%), as well as being calculated from the geometry and current of the coils. From these three measures, the fields are determined to be 8.88(9) and 25.62(24) G, which lead to shifts of 15.6(0.3) kHz and 129.8(2.4) kHz, as shown in Table I.

Another important uncertainty is due to the possible variation of microwave power as the microwave frequency is tuned. The microwaves are produced by a Wiltron 68169B signal generator, followed by a 1-W DBS Microwave power amplifier. The amplifier is specified to have power variations of less than 0.1 D over 100 MHz, and is confirmed to have variations of less than 0.1%/MHz in the frequency range of interest. The power amplifier has a hermetically sealed WR28 waveguide output that serves as the vacuum seal for feeding the microwaves into the vacuum chamber. The amplifier is followed by a 27.4-cm straight section of waveguide, with the 1.6-mm hole being 16.3 cm below the amplifier. After this section, a microwave terminator with a voltage standing-wave ratio of 1.004 absorbs the microwave power. Variations of microwave power versus frequency can also be caused by microwave reflections from the various components within the microwave system. These reflected waves interfere with the incident microwave power, and the degree of interference varies slightly as the frequency (and thus wavelength) of the microwaves is tuned. The maximum variation that could result from the reflections in our microwave system is 0.04%/MHz. As a further test of reflections, data were taken with an extra 1/4-wave section of waveguide added before or after the 27.4-cm section. This section serves to reverse the sign of the interference and thus reverse the sign of the shift in our resonance. The consistency between these measurements confirms that the effect of the reflected waves is small. An uncertainty of 3.5 kHz is included in Table I to account for both types of possible power variations.

Some additional data were taken at one-half microwave power, with 10 times higher pressure in our vacuum system (2×10^{-6} Torr as compared to 2×10^{-7} Torr), or with the excitation laser set to excite from the $2\,^3S_1$ $m=-1$ state instead of the $m=+1$ state. Also data were taken with the waveguide section reversed. In all cases, there is no expected shift and no shift is found. The dc Stark shift rate for this interval is approximately 10 kHz/(kV/cm)^2. We estimate that the dc fields near the waveguide are less than 10 V/cm, leading to a negligible shift. A Cs clock standard obtained from the GPS satellite system is used to calibrate our microwave frequencies with negligible uncertainty.

Table I shows that the measured value for the interval is consistent for the two magnetic fields, for the two numbers of 25-μm wires, for the different excitation-laser powers, and for the two repetitions of the data set. The final measured result for the interval is 29 616.966(13) MHz. This is the most precise microwave measurement of the interval and it does not agree well with the previous [3] microwave measurement of 29 616.864(36) MHz. The result is in agreement with two recent laser measurements of the interval: 29 616.962(4) [4] and 29 616.981(25) [25] (and is within two standard deviations of a third measurement: 29 616.936(8) [16]); and thus resolves the previous discrepancy between laser and microwave measurements.

At present, our measurement accuracy is almost entirely dominated by the effects of the microwave leakage fields. We intend to solve this leakage-field problem [11]. Our statistical uncertainty is below 1 kHz for two weeks of data collection and can be improved by (1) increasing the microwave power and thus increasing the induced transition probability above the present 2% and (2) by improving our fluorescence collection optics to increase the collection efficiency. These two improvements will not only greatly reduce our statistical uncertainty, but will also allow us to perform the extensive systematic tests that will be necessary for a sub-kHz measurement of the interval.

The present best theory [2] of 29 616.974(20) is in good agreement with the present measurement. The uncertainty of 20 kHz is due to as-yet uncalculated terms. These terms are presently being calculated [12], and it is expected that the theoretical uncertainty will also soon be reduced to the sub-kHz level. A comparison of theory and experiment at the 1-kHz level will give a new determination of the fine-structure constant accurate to 17 ppb.

This work is supported by the Natural Sciences and Engineering Research Council of Canada. We would like to thank the National Research Council for use of their microwave testing facilities and would like to thank N. E. Rothery and R. T. Ross for their contributions to the measurement.

[1] J. Daley, M. Douglas, L. Hambro, and N. M. Knoll, Phys. Rev. Lett. **29**, 12 (1972).

[2] T. Zhang and G. W. F. Drake, Phys. Rev. A **54**, 4882 (1996).

[3] F. M. J. Pichanick, R. D. Swift, C. E. Johnson, and V. W. Hughes, Phys. Rev. **169**, 55 (1968); A. Kponou, V. W. Hughes, C. E. Johnson, S. A. Lewis, and F. M. J. Pichanick, Phys. Rev. A **24**, 264 (1981); W. Frieze, E. A. Hinds, V. W. Hughes, and F. M. J. Pichanick, *ibid.* **24**, 279 (1981).

[4] D. Shiner, R. Dixon, and P. Zhao, Phys. Rev. Lett. **72**, 1802 (1994); D. L. Shiner and R. Dixon, IEEE Trans Instrum. Meas. **44**, 518 (1995).

[5] M. Prevedelli, P. Cancio, G. Giusfredi, F. S. Pavone, and M. Inguscio, Opt. Commun. **125**, 231 (1996).

[6] Jesse Wen and G. Gabrielse, Ph.D. thesis, Harvard University, 1996 (unpublished).

[7] W. Rooijakkers, W. Hogervorst, and W. Vassen, Opt. Commun. **123**, 321 (1996); D. W. Fahey, W. F. Parks, and L. D. Schearer, J. Phys. E **13**, 381 (1980).

[8] W. E. Lamb, Phys. Rev. **105**, 559 (1957).

[9] G. W. F. Drake, in *Handbook of Atomic, Molecular and Optical Physics*, edited by G. W. F. Drake (AIP Press, Woodbury, NY, 1996), Chap. 11.

[10] Z.-C. Yan and G. W. F. Drake, Phys. Rev. A **50**, R1980 (1994); S. A. Lewis, F. M. J. Pichanick, and V. W. Hughes, *ibid.* **2**, 86 (1970).

[11] The leakage fields could be better contained using a fine screen, or, alternatively, the laser excitation could take place inside of the waveguide, so long as the microwaves are switched off while the laser excitation takes place.

[12] G. W. F. Drake (private communication).